Table S1. Sequences of A, B, and C domains for constructing the ICK scaffold library

No	Domain_A	link1	Domain_B	link2	Domain_C
1	AACLGMFES	C	**ADSDDCCETFH**	C	ALGICMPR
2	ACGQFWWK	C	AWFSGESCCTGI	C	ATTGRFRYLCKYQI
3	ACKGVFDA	C	DEERKCCEGLV	C	DRRDQWCKWNPW
4	ACREWLGG	C	DENDPRCCSGLV	C	ELWCKYNL
5	ADCGWLFHS	C	DGKSTFCCSGFN	C	ERSSPWCKIDIW
6	CAAEGIP	C	DGKSTFCCSGYN	C	HLWCKYK
7	CGGWMAK	C	DPDNDKCCEGYK	C	HSLFSYCAWDLTFSD
8	CIGEGVP	C	DPKNDKCCKNYT	C	HSNYEWCIWDGTFSK
9	CMGYDIH	C	DPKNDKCCPNRV	C	HSNYEWCVWDGT
10	DCAGYMRE	C	DPNNDKCCPNRE	C	HSRWDWCIWDGTF
11	DCGTIWHY	C	DPNNDKCCPNRV	C	HSYWEWCLWDGSF
12	DCLGFLWK	C	DPNPVKDLPCCSGLA	C	ICSGXNWK
13	DCLGLFWI	C	DSARKCCEGLV	C	ISTKVNYYCRPDRGP
14	DCLGWFKG	C	DSERKCCEDMV	C	KAFVLHCYRN
15	DCLGWFKS	C	DSERKCCEGMV	C	KDVLYYCAWDGTF
16	DCRALYGG	C	DSERKCCEGYV	C	KEKWPITYKICVWDRTF
17	DCRKMFGG	C	DSKRACCEGLR	C	KELSIWDSRCL
18	DCTRMFGA	C	DSKRKCCEDMV	C	KFRDKYCAWDFTFS
19	DCVRFWGK	C	DSNADCCEGYV	C	KGPSPKQKKCTRP
20	DDCGGLFSG	C	DSTLDCCKHLS	C	KGRFVNTWPTFCLV
21	DDCGKLFSG	C	DTNADCCEGYV	C	KIGLYLCIWSP
22	DDCGTLFSG	C	DTSKDCCEGYV	C	KLWCRKIIG
23	DDCLGMFSS	C	DYNNGCCSGYV	C	KLWCRYERTW
24	DDDCGWIMDD	C	EKDEHCCEHLG	C	KMGLDYCAWDGTF
25	DGECGGFWWK	C	EKDSDCCEHLG	C	KMGLYYCAWDGTF
26	ECGKFMWK	C	ESNADCCENWA	C	KPTLKYCAWDGT
27	ECGTLFSG	C	FRDKECCKGLT	C	KPTLKYCAWDGTF
28	ECKGFGKS	C	GAGKPTCCSGYD	C	KPTSKYCAWDGTI
29	ECKKLFGG	C	GEGKPPCCANFA	C	KQKWPFYCAWDWSF
30	ECKWYLGD	C	GRGKPPCCKGYA	C	KRRGTNAEKRCR
31	ECKYLWGT	C	GSGKPACCPKYV	C	KRRGTNIEKRCR
32	ECLEIFKA	C	GTDQSECCEGWK	C	KRTFNYCAWDGSFSK
33	ECLGFGKG	C	HPGQPPCCSGLA	C	KSKWPRNICVWDGSV
34	ECRKMFGG	C	KADNDCCGKK	C	KTTGIVKLCRW
35	ECRWLFGG	C	KAHEDCCEHLR	C	**KWVFFTSKFMCRRVWGKD**
36	ECRWYLGG	C	KEDSECCEHLQ	C	LKPTLHGIWYKHHYCYTQ

37	ECRYFWGE	**C**	KEKLCCSGYV	**C**	LKPTLHGIWYKSYYCYKK
38	ECRYLFGG	**C**	KENKDCCSKK	**C**	NGNTVYRCA
39	ECRYWLGG	**C**	KKDKECCGWNI	**C**	NKKHGWCGWDGTF
40	ECRYWLGT	**C**	KNKKECCGWNA	**C**	NKKYWHCGWDGTF
41	ECTKFLGG	**C**	KNSNDCCKDLV	**C**	NRKHKWCKYKLW
42	ECTKLLGG	**C**	KSDENCCKKFK	**C**	NRRDKWCKYKLW
43	EDCIPKWKG	**C**	KSTSDCCEHLS	**C**	NSRDKWCKVLL
44	EGECGGFWWK	**C**	KTTADCCKHLA	**C**	QLWCKKRL
45	GACRWFLGG	**C**	KTTADCCKHLG	**C**	QPAIKWCIWSP
46	GCANAYKS	**C**	KTTSDCCKHLG	**C**	QSRIANMWPTFCLV
47	GCGGLMAG	**C**	NALSGPRCCSGLK	**C**	QSRIANMWPTFCSQ
48	GCGGLMDG	**C**	NDEMVCCEHLV	**C**	RKKWPYHCGWDGTF
49	GCGTMWSP	**C**	NGPHTCCWGYNGYKKA	**C**	RKKWPYHCVWDWTV
50	GCIPSFGE	**C**	NPDNDKCCEGRK	**C**	RLWCKKII
51	GCKGFGDS	**C**	NPNDDKCCRPKLK	**C**	RLWCKKKIEEG
52	GCKLTFWK	**C**	NPSNDKCCRPNLV	**C**	RLWCKKKIEW
53	GCLEFWWK	**C**	NPSNDQCCKSANLV	**C**	RLWCKKKLW
54	GCLGDK	**C**	NPSNDQCCKSSKLV	**C**	RLWCKKRL
55	GCNRKNKK	**C**	NPSNDQCCKSSNLV	**C**	RLWCKLDW
56	GCQKFFWT	**C**	NSDADCCRYGER	**C**	RLWCKRIINM
57	GDCLPHLKL	**C**	NSDKECCKGLR	**C**	RLWCKYKL
58	GDCLPHLKR	**C**	NYMDDKCCPGYK	**C**	RRAKPSWCGWDFTF
59	GGCLPHNRF	**C**	PKKAPCCGRLE	**C**	RRAKPSWCGWDFTV
60	GVDKAGCRYMFGG	**C**	PYHESCCSGS	**C**	RRTLPTYCAWDLTFP
61	GVDKEGCRKLLGG	**C**	PYNEHCCSGS	**C**	RSDGKYCAWDGTF
62	IACAPRFSI	**C**	PYNENCCSKS	**C**	RSDWKYCAWDGTFS
63	IACAPRFSL	**C**	PYNENCCSQS	**C**	RSRDQWCKYKLW
64	IACAPRGLL	**C**	PYNESCCSGS	**C**	RVRDQWCKYKLW
65	KCLPPGKP	**C**	PYSKYCCSGS	**C**	SDKHKWCKWKL
66	LCSREGEF	**C**	QPNTQPCCNNAEEEQTIN	**C**	SHNKCT
67	QCGEFMWK	**C**	RENKDCCSKK	**C**	SKLFKLCNFSF
68	RCIEEGKW	**C**	RRDSDCCPHLG	**C**	SKTGFVKNICKYEM
69	SAVCIPSGQP	**C**	SAGQTCCKHLV	**C**	SKTWGWCAVEAP
70	SCKLTFWR	**C**	SEDSECCPHLG	**C**	SPKHGWCVWDWTFRK
71	SECRWFMGG	**C**	SKDADCCAHLE	**C**	SPKWGLCNFPMP
72	SEKDCIKHLQR	**C**	SKHEDCCAHLA	**C**	SPRWGWCIYSTRGGR
73	SFCIPFKP	**C**	SKTGDCCSHLS	**C**	SPTWKWCVLKSPGRR
74	SPTCIPSGQP	**C**	SQDGDCCKHLQ	**C**	SPTWKWCVYARP
75	SPTCIPTGQP	**C**	SQTSDCCPHLA	**C**	SQHRLCSVKA
76	SPTCIRSGQP	**C**	SSDKPCCSGYY	**C**	SRKDKWCKYQI
77	SPVCTPSGQP	**C**	SSTSDCCKHLS	**C**	SRKHRWCKYEI

78	**SSTCIPSGQP**	**C**	STEKPCCDNFS	**C**	SRKTRWCKYQI
79	SSTCIRTDQP	**C**	STHADCCEGFI	**C**	SRQLCKYVIDW
80	STCTPTDQP	**C**	SVDSDCCAHLG	**C**	SRRDRWCKYDL
81	SVCIPSGQP	**C**	SVHSDCCAHLG	**C**	SRRDRWCKYYL
82	TCRYLFGG	**C**	SVNDDCCPRLG	**C**	SRRGTNPEKRCR
83	TCYDIGEL	**C**	TDRLPCCFGLE	**C**	SRRHGWCVWDGTFS
84	VCRGYGLP	**C**	TIDDDCCPHLG	**C**	SRTWKWCVLAGPW
85	YCQKWLWT	**C**	TKDEDCCKHLA	**C**	SSKHKWCKVYL
86	YCQKWMWT	**C**	TKDSECCPHLG	**C**	SSRWKWCVLASPF
87	CKQADEP	**C**	TPEKNDCCQRLY	**C**	SSRWKWCVLPAPW
88	ACRKKWEY	**C**	TPGKNECCPNRV	**C**	TFKENENGNTVKRCD
89	DDDCEPPGNF	**C**	TPGKNECCPNYA	**C**	TFKTNENGNTVKRCD
90	VKPCRKEGQL	**C**	TSDSDCCPNWV	**C**	TGLCIPP
91	WCKQSGEM	**C**	TTSSECCAHLG	**C**	TRFNVCGK
92	CLSGGEV	**C**	VNRHGDCCEGLE	**C**	TWPTEICID
93	GKPCHEEGQL	**C**	VPGKNECCSGYA	**C**	TYKANENGNQVKRCD
94	CIPFLHP	**C**	YGATQKIPCCGV	**C**	TYKENENGNTVKRCD
95	ACSKKWEY	**C**	YKLRKCCAGFY	**C**	TYKENENGNTVQRCD
96		**C**	DVFSLDCCTGI	**C**	TYKTNENGNSVQRCD
97		**C**	IVPIIGFIYCCPGLI	**C**	VKTSGYWWYKKTYCRRKS
98		**C**	GMIKIGPPCCSGW	**C**	WKRRRSFEVCVPKTPKT
99		**C**	DPIFQNCCRGWN	**C**	LGVCMW
100		**C**	NVLDQNCCDGY	**C**	FFACA
101		**C**	DFLFPKCCNY	**C**	VLFCV
102		**C**	DPFLQNCCLGWN	**C**	IVFVCT
103		**C**	TFFFPDCCNSI	**C**	ILLFCS
104		**C**	IVPILGFVYCCPGLI	**C**	VFVCI
105		**C**		**C**	AQFICL
106		**C**		**C**	GPFVCV

The public database UniProt (www.uniprot.org) was evaluated for sequences homologous to ProTx-II and bearing the same predicted pattern of disulfide bridges, as described in *Materials and Methods*. This table lists the unique domains in the 110 parent sequences. Domains A (95), B (104), and C (106) segments were joined at the 2nd and 5th Cys residues. In bold are three segments from parental toxin Omega-AcTx-Hv1b, JZTX21 and Neurotoxin Hm2, that forms novel toxin C6.

Table S2. Stoichiometry of hHv1 and ΔhHv1 channels formed with TFP encoded subunits.

	Subunits expressed	
Ananlysis	hHv1-TFP	ΔhHv1-TFP
Determined subunits stoichiometry in channels	2	1
Particles studied (*N*)	114	112
Particles with		
One step	11	100
Two steps	100	9
Three steps	1	2
Four steps	2	1
Confidence	0.999	NA
θ	0.95	NA
θ+ 1	0.63	NA

TFP-tagged hHv1 or ΔhHv1 subunits were expressed in HEK293T cells and studied by smTIRF (*Materials and Methods*). The number of photobleaching steps observed for TFP fluorophore in each single fluorescent spot reports on the stoichiometry of channels. WT hHv1-TFP channels are dimers and ΔhHv1-TFP channels are monomeric. Analysis was performed according to methods described by Hines. The statistical confidence in the null hypotheses that hHv1 forms dimers was assessed to be greater than 0.999. Prebleaching and variance in quantum efficiency reduce the probability of observing each possible bleaching event (θ). θ is calculated from the value of n and the distribution of the photobleaching data per Hines. θ is decreased when the distribution is altered to estimate the possibility that higher numbers of missed bleaching steps, for example θ + 1, indicating that this stoichiometry is less likely. NA indicates not applicable.

Table S3. Analysis of single molecule photobleaching for smTIRF experiments with ΔhHv1 and C6.

	Subunits expressed and fluorescence labeled C6 peptide applied					
	ΔHv1-TFP (monomer)					
Analysis	With 0.01 nM TAMRA-C6	With 0.1 nM TAMRA-C6	With 1 nM TAMRA-C6	With 10 nM TAMRA-C6	With 100 nM TAMRA-C6	With 1 μM TAMRA-C6
Manders' coefficient	0.08± 0.01	0.12 ± 0.01	0.50 ± 0.05	0.83± 0.04	0.9± 0.06	0.93 ± 0.06
Particles studied	50	50	112	50	50	100
Particles with one TFP bleaching steps	45	45	100	47	46	91
Colocalized particles (N)	4	6	51	40	41	84
Particles with (TAMRA bleaching)						
One step (n)	4	6	51	40	41	84
Two steps	0	0	0	0	0	0
Three steps	0	0	0	0	0	0
Four steps	0	0	0	0	0	0
Number of colocalized ΔhHv1 with one TAMRA bleaching steps (n/N, %)	4/4 (100%)	6/6 (100%)	51/51 (100%)	40/40 (100%)	41/41 (100%)	84/84 (100%)

ΔHv1-TFP was expressed in HEK293T cells and incubated with varying concentrations of TAMRA-C6 toxin for reaching equilibrium. Mean Manders' coefficient for colocalization were determined as described in the *Materials and Methods*. Data were reported and analyzed as in Table 1.

Fig. S1. Binding of TAMRA-C6 to ΔHv1 monomeric channel.

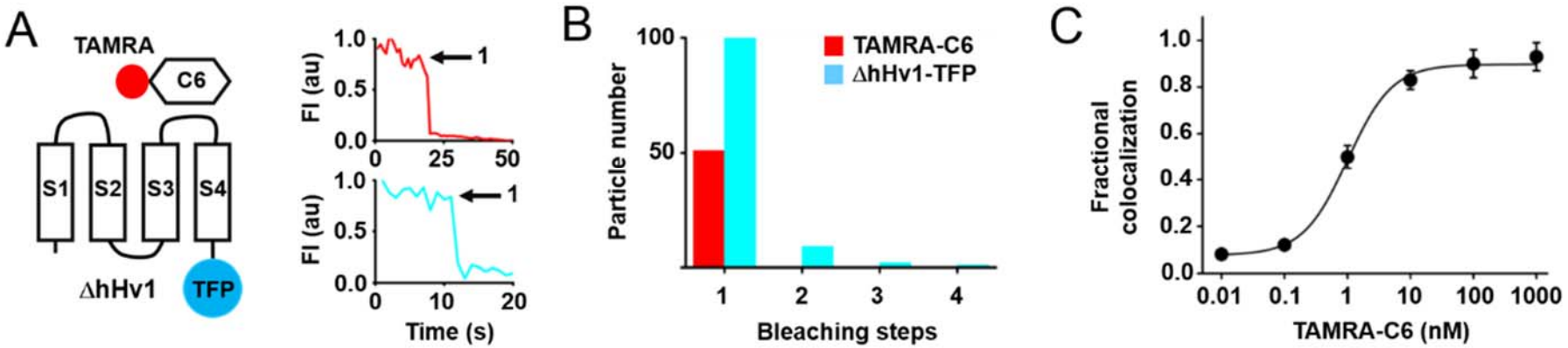

C6 peptide was synthesized and labeled with red fluorophore carboxytetramethylrhodamine (TAMRA-C6). Its interaction with ΔhHv1 tagged with teal fluorescent protein (ΔhHv1-TFP) was studied in HEK293T cells by smTIRF microscopy as described in *Materials and Methods*.

(A) Cartoon showing one TAMRA-C6 peptide binding on monomeric hHv1 channel (ΔhHv1-TFP), which was constructed as described in *Materials and Methods*. Simultaneous photobleaching time course for representative colocalized particles with both ΔhHv1-TFP and TAMRA-C6 shows one stepwise change in fluorescence intensity.

(B) Histogram of photobleaching steps for ΔhHv1-TFP (teal bars) simultaneously photobleached with 1 nM TAMRA-C6 (red bars). 89% of studied particles with ΔHv1–TFP were bleached in 1 step. Among all colocalized particles containing both fluorescent colors, 100% have one TAMRA-C6 bleaching step (Table S3).

(C) Dose–response for hHv1 titrated with TAMRA-C6 at increasing concentrations. Solid lines correspond to fit Hill relationship, yields K_d = 1.08 ± 0.13 nM and a Hill coefficient of 1.02 ± 0.14. Each point represents mean ± SEM for 5 cells studied in each condition.

Fig. S2. C6 does not inhibit rNav1.4 and hKv2.1.

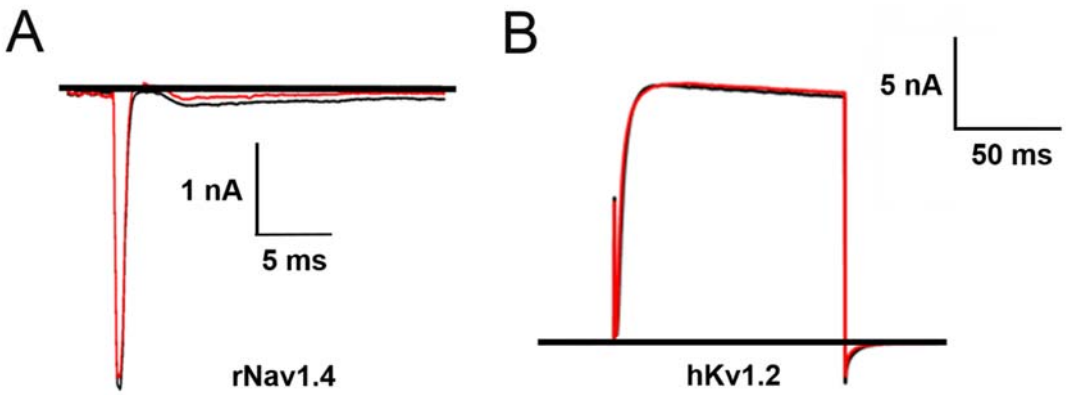

Channels were studied in HEK293T cells using whole cell voltage clamp as described in the *Materials and Methods*.

(A) rNav1.4 was expressed in HEK293T, and studied using 30 ms pulse to 0 mV from a holding voltage of -100 mV with 10 s interval. 1 μM C6 (red trace) was applied after control pulses and shows not inhibition comparing to control current before application (black trace).

(B) hKv2.1 was expressed in HEK293T, and studied using 250 ms pulse to 40 mV from a holding voltage of -80 mV with 10 s interval. 1 μM C6 (red trace) was applied after control pulses and shows not inhibition comparing to control current before application (black trace).

Fig. S3. The S1-S2 loop of hHv1 is not the major binding epitope for C6.

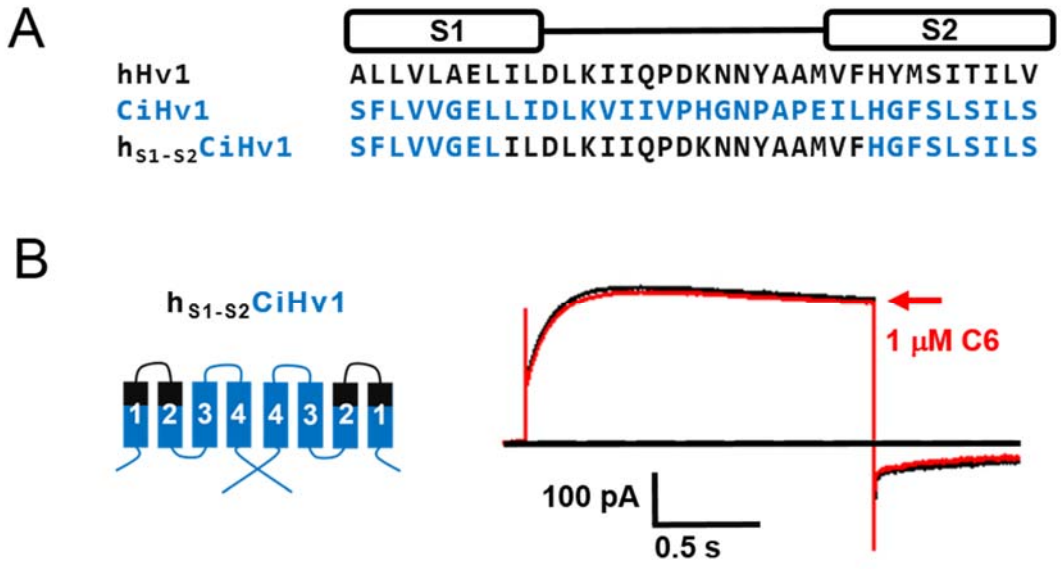

Channels were studied in HEK293T cells using whole cell voltage clamp as described in the *Materials and Methods*.

(A) Sequence alignment of CiHv1 (blue), hHv1 (black) and $h_{S1\text{-}S2}$CiHv1 chimera transplanting the S1-S2 loop of hHv1 into CiHv1.

(B) Representative current traces for $h_{S1\text{-}S2}$CiHv1 with 1 µM C6 (red) or without C6 (black). C6 does not block CiHv1 (Fig. 4*B*) or $h_{S1\text{-}S2}$CiHv1 at 1 µM.

Fig. S4. The S3-S4 loop of hHv1 confer C6 inhibition on hKv2.1.

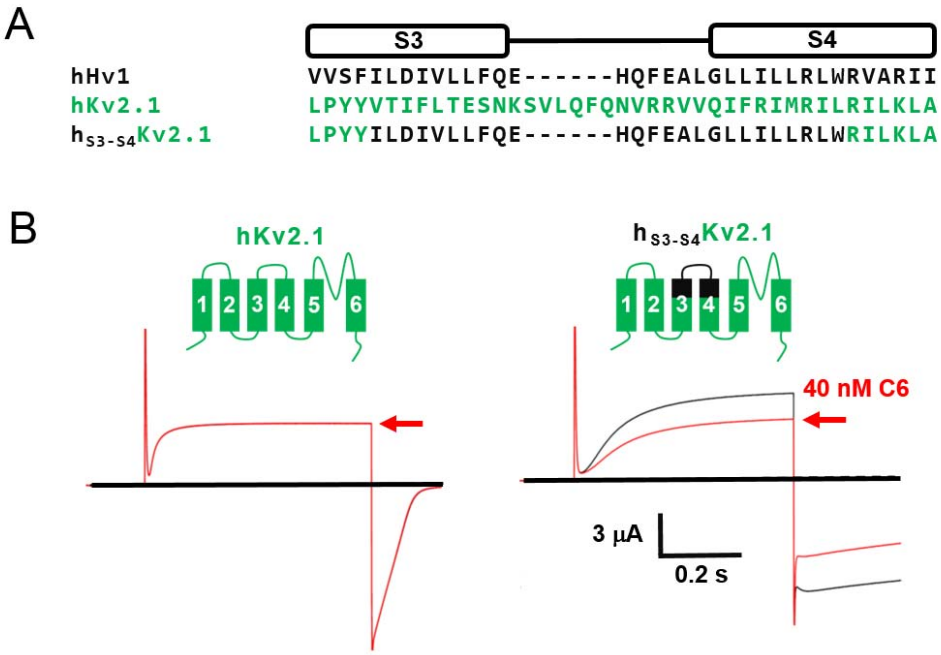

Channels were expressed in *Xenopus* oocytes and studied by TEVC with a holding voltage of -80 mV and 0.5 s steps to 0 mV every 10 s, as described in *Materials and Methods*.

(A) Sequence alignment of hKv2.1 (green), hHv1 (black) and $h_{S1\text{-}S2}$Kv2.1 chimera transplanting the S1-S2 loop of hHv1 into hKv2.1.

(B) Representative current trace for hKv2.1 and $h_{S1\text{-}S2}$Kv2.1 with 40 nM C6 (red) or without C6 application (black).

Fig. S5. C6 did not suppress the acrosome reaction of capacitated sperm.

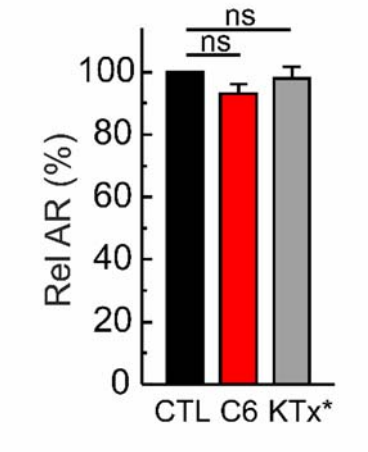

Human spermatozoa were collected and capacitated as described in *Methods and Materials*, and then incubated with or without peptides for 30 min. The acrosome reaction was triggered subsequently by progesterone and measured the same as in Fig. 5C. CTL indicates control with no added peptide.

Fig. S6. C6 did not affect protein tyrosine phosphorylation in sperm.

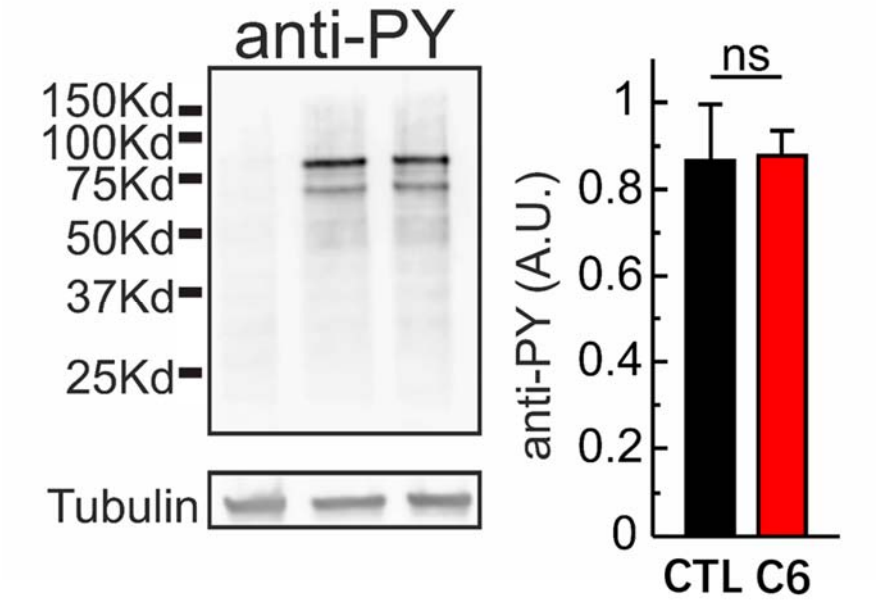

Human sperm were incubated with or without 20 μM C6 before lysis. Proteins were extracted and analyzed by Western blot using human monoclonal anti-phosphotyrosine antibodies as probe, as described in *Materials and Methods*.. C6 has no effect on the phosphorylation of protein tyrosine kinase.

Fig. S7. C6 does not inhibit Catsper in human sperm directly.

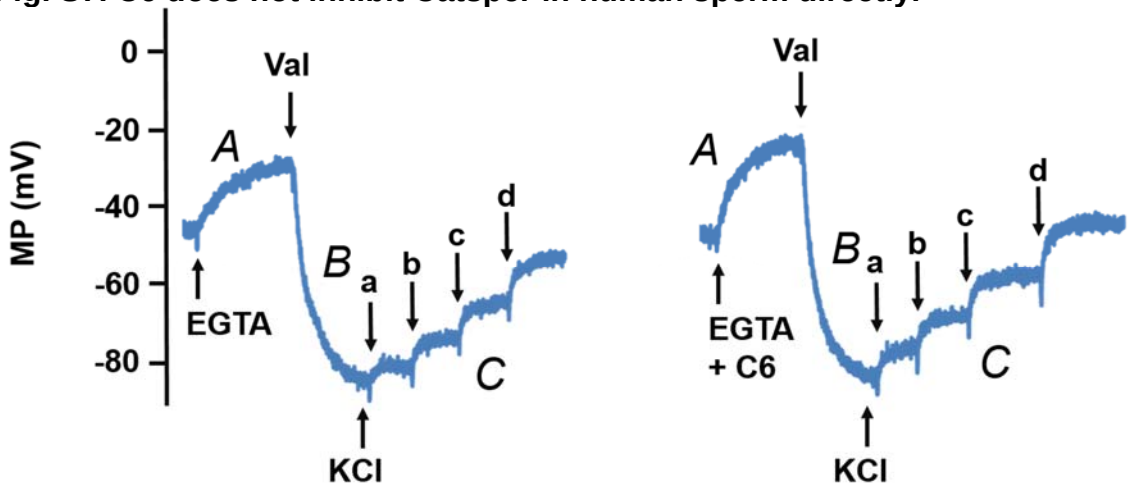

The effect of C6 on CatSper inhuman sperm was evaluated by measuring changes in membrane potential (MP) in HTF media after adding 3.5 mM EGTA, which chelates external Ca^{2+} and allows Na^{+} to permeate through Ca^{2+} permeable channels, depolarizing the sperm. After adding EGTA, MP rises 20 ± 2 mV (phase A) due to Na^{+} influx in control sperm. Similarly, with 20 µM C6, EGTA chelation leads to a rise in the MP of 22 ± 3 mV. Valinomycin decreases MP ~60 mV in control sperm due to K^{+} efflux and the effect is similar in sperm incubated with C6 (phase B). Four subsequent additions of KCl moves the MP in correspondence with the Nernst potential for potassium distribution across the plasma membrane (phase C). The initial suspension contains 4.7 mM KCl, and the subsequent KCl additions resulted in final concentrations (mM KCl) in the sperm suspension of 1.2 (a), 2.5 (b), 5 (c), and 10 (d), which correspond to MP of -87, -80, -71, -58, and -44 mV.